

## Selective and Simultaneous Detection of Dopamine using Gr-TiO<sub>2</sub> Modified Electrode

T. Jyothish kumar<sup>1\*</sup>, K.B. Manoj<sup>1</sup>, K. Sreevalsan<sup>1</sup>, V. Anithakumary<sup>2</sup>

<sup>1</sup>(Department of Chemistry, S.N.College, Kollam, University of Kerala)

<sup>2</sup>(Department of Chemistry, S.N.College for Women, Kollam, University of Kerala)

\*Corresponding author: jyothishsree@gmail.com

---

**Abstract:** A novel voltametric sensor based on Graphene-TiO<sub>2</sub> was developed. The graphene-TiO<sub>2</sub> nanocomposite was prepared by the hydrothermal treatment. It provides an efficient and facile approach to yield nanocomposite with TiO<sub>2</sub> nanoparticles uniformly embedded on graphene substrate. The crystallinity and crystalline size were examined by XRD and TEM. The surface morphology of the nanocomposite is examined by SEM. The crystalline size of the as prepared nanocomposite was 17nm. The electrochemical behavior of Dopamine was investigated with this sensor. The Gr-TiO<sub>2</sub> modified electrode exhibited a linear response in differential pulse voltametry, with the detection limit of 54nM.

**Key words:** Dopamine, Graphene, Graphene-TiO<sub>2</sub> nano composite, Hydrothermal method.

### I. Introduction

Graphene is a 2D sheet of sp<sup>2</sup> bonded carbon atoms, densely packed in a honeycomb crystal lattice structure whereby each of these layers is held together by weak Vander Waals forces [1]. The most important property of graphene is its excellent electrical conductivity. The various forms of graphene-based materials include thermally reduced graphene oxide (TRGO), chemically reduced graphene oxide (CRGO), and electrochemically reduced graphene oxide (ERGO), contains oxygen-containing functional groups and certain amounts of defects [2–4]. The rapid electron transfer takes place at the surface of edge planes and defects when compared to the basal planes for the electrochemical sensors fabricated with graphene based materials [5–7]. The presence of these structural defects in the chemically modified graphene can be exploited for electrochemical sensor applications. The presence of oxygen-containing functional groups in the graphene-based materials play a vital role in the electrochemical sensors, which makes the adsorption and preconcentration of the redox species (which is of our analytical interest) and effectively catalyse the redox reactions. In addition, the presence of these functional groups makes an effective functionalization with various biomolecules and polymers for applications [8–10]. The functionalization of these graphene based materials with specific functional groups can enable the use of these excellent materials for electrochemical sensor applications with specific analytes. The functionalized graphene materials also make fast electron transfer by pre-concentrating the target analytes at the electrode surface.

Graphene-based nanocomposites with semiconductor and metal nanoparticles have received increasing attention due to their remarkable electrocatalytic, electrochemical sensing and electrochemical energy conversion properties [11–22]. The remarkable properties of metal nanoparticles incorporated on graphene depicts high electrocatalytic activity, excellent conductivity, and selectivity which makes metal nanostructures decorated on graphene an ideal choice to be used as an active material in electrochemical sensors.

Due to its good biocompatibility and high conductivity, TiO<sub>2</sub> has been widely used in the fabrication of electrochemical biosensors [23–29]. In these biosensors, TiO<sub>2</sub> was employed as support matrix for immobilizing enzymes, which can facilitate the direct electron transfer and enhance the catalytic activity of enzymes.

Dopamine, a neurotransmitter plays a fundamental role in mood regulation, cognition, addiction and reward. Regulation of dopamine has a crucial role in our mental and physical health. Dopamine is present in the body in very low concentrations. Deficiency or imbalance of this neurotransmitter in the body leads to several neurological disorders such as Parkinson's disease and Schizophrenia [30]. If the DA produced in the central nervous system is abnormal, it is a sign of an underlying condition of a neurological disorder in the human body. Diseases such as Parkinson's disease, attention deficit hyperactivity disorder (ADHD), schizophrenia, restless leg syndrome and HIV infection causes due to the low level of DA. DA is also highly linked with the reward mechanism in the brain. Since DA acts as a neurotransmitter which is vital for message transfer functions, use of illegal drugs or substance abuse such as heroin, cocaine, nicotine and alcohol blocks the DA transport that inhibits

the re-uptake of DA and eventually increases the DA levels, causing an increased risk of depression and drug addiction.

In the past, various analytical methods have been set up and pronounced for the detection of DA. This includes the capillary electrophoresis mass spectrometry approach, chromatography, fluorimetry, speedy liquid chromatography/tandem mass spectrometry (LC-MS/MS), and chemiluminescence [31; 32; 33] although these techniques offer high sensitivity in the detection of DA, they have numerous drawbacks. They require a complicated machine, long time-intake, high cost, and take a tremendous big amount of workspace. Consequently, the detection of DA by using electrochemical technique is a greater appropriate approach in comparing the low concentration of DA beneath physiological situations. This method provides beneficial characteristics of simplicity, quick time delay, value-effective, right selectivity, and actual-time detection without comprising its sensitivity talents [34; 35; 36].

Diverse methods like capillary electrophoresis [37], fluorometry [38,39], chromatography [40], spectrophotometry [41] and chemiluminescence [42] are being employed for the detection of dopamine. Despite the fact that these strategies can provide correct selectivity and low restriction of detection, they frequently require complex pre treatment steps and costly instrumentation. Hence alternative methods for the detection of dopamine are necessary. In contrast to spectroscopic chromatographic contraptions, electrochemical sensors may be effortlessly adapted for detecting a wide variety of analytes while closing inexpensive. Ease of electrode fabrication through the use of position changes, the tremendous possibility to tailor the change on the operating electrode and discover its novel electrocatalytic outcomes toward the analytes and fast reaction are different striking advantages of electrochemical sensors. Additionally those sensors are capable of being integrated into robust, portable or miniaturised devices permitting tailoring for unique programs. So it will be promising to apply electrochemical era and develop novel sensors as the call for of sensitive, rapid and selective determination of analytes increases.

The presence of structural defects within the chemically modified graphene can be exploited for electrochemical sensor packages. The presence of oxygen-containing purposeful groups in the Graphene based materials play a vital function in the electrochemical sensors, which makes the adsorption and preconcentration of the redox species (that is of our analytical Interest) and correctly catalyse the redox reactions. Further, the presence of those functional organizations makes an effective functionalization with diverse biomolecules and polymers for Programs [43; 44; 45]. The functionalization of those graphene based materials with specific functional organizations can allow the use of those incredible substances for electrochemical sensor applications with specific analytes. The functionalized graphene materials additionally make speedy electron transfer with the aid of pre-concentrating analytes at the electrode surface. Among those biomolecules, DA is the most crucial biomolecule and it's miles extra oxygen was detected by means of graphene (functionalized and n doped) and their composites with metals, steel oxides, Steel-natural frameworks, Polymers, Clay, Zeolite, and Carbonaceous substances.

Making composite with metals, metal oxides, metallic organic Frameworks, polymers, clay, zeolite, and carbonaceous materials, Graphene acquires wonderful electrocatalytic residences which cause the higher detection of DA in the presence of Interfering species. There are different graphene-based composite materials with metal [46], steel Oxides [47], and polymer [48] with improved sensitivity and electrocatalytic interest. In 2011, graphene-carbonaceous materials and graphene-clay composites were used as alternative electrode modifier substances for the detection of DA [49; 50]. Other than composite materials, the function of functionalized Graphene for the detection of DA was additionally investigated in the same period [51]. Following this, a brand new field emerges in knowledge N-doped graphene materials for the detection of DA [52] in 2012. MOF with porous and huge floor area was incorporated into graphene substances that open up a new possibility for the improvement of sensitive DA sensors.

## **II. Experimental**

### *2.1. Chemicals*

Graphite powder (320 mesh, spectrum pure) was purchased from Sinopharm Chemical Reagent Co., Ltd. Titanium isopropoxide (Ti(OiPr)<sub>4</sub>) was obtained from Sigma aldrich. Other chemicals used in this study were of analytical grade. All solutions were prepared with double distilled water. All the prepared samples were analyzed with PXRD, SEM, Cyclic voltammetry (CV) and differential pulse voltammograms (DPVs) were recorded using CHI 604D electrochemical analyzer, in a conventional three-electrode cell. A platinum wire, Ag/AgCl and a glassy carbon electrode (GCE) modified with the composite were used as counter electrode, reference electrode and working electrode, respectively. All experiments were carried out at room temperature.

a. *Preparation of GR/TiO<sub>2</sub> nanocomposite*

Graphene oxide was synthesized from graphite powder by the improved Hummers method [13]. Suitable amount of graphite powder was taken in a RB flask. To this required quantity of cold concentrated mixture of H<sub>2</sub>SO<sub>4</sub> and orthophosphoric acid was added. The mixture was stirred for about 2 hours at room temperature. After the stirring, add KMnO<sub>4</sub> very slowly under stirring kept the temperature of the mixture below 20°C. Then the reaction was heated to 50°C and kept under stirring for 6 hours. Then it was cooled and poured into ice containing 30% H<sub>2</sub>O<sub>2</sub>. The mixture was then centrifuged, washed and dried. Graphene was prepared by the thermal exfoliation of graphene oxide. Hydrothermal preparation of GR/TiO<sub>2</sub> nanocomposite was carried out by the following procedure. Titanium isopropoxide (0.2 mL) was mixed with graphene (50 mg) in a 25mL Teflon-sealed autoclave, and H<sub>2</sub>SO<sub>4</sub> (1 M, 2mL) was then added. The resultant mixture was ultrasonicated for 10 min, and then the autoclave was kept in oven maintained at 170 °C for 24 h. The final product was isolated by filtration, rinsed thoroughly with deionized water and methanol, and dried in vacuum. The GR/TiO<sub>2</sub> nanocomposite was obtained in the form of black powder.

b. *Preparation of Modified electrode*

The as Prepared Gr-TiO<sub>2</sub> nanocomposite(1.5mg) was dispersed in 1 ml DMF to form a homogenous suspension. The Gr-TiO<sub>2</sub> modified GCE was prepared by dropping 7microL of the suspension on the surface of freshly polished GCE and dried .

### III. Results and Discussion

#### 3.1. Characterization of Graphite oxide and Reduced Graphene oxide

Figure 3.1.1 shows the XRD patterns of Graphene oxide prepared by the Modified Hummers method [13]. Figure 3.1.2 depicts the XRD pattern of Graphene prepared by the thermal exfoliation of graphene oxide.

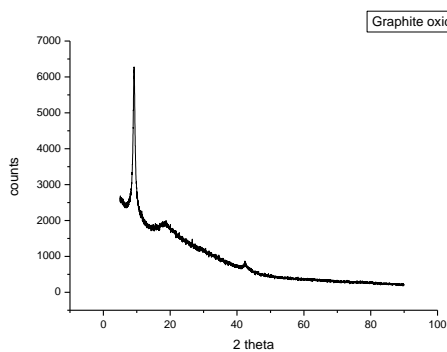


Fig 3.1.1: XRD of Graphene Oxide

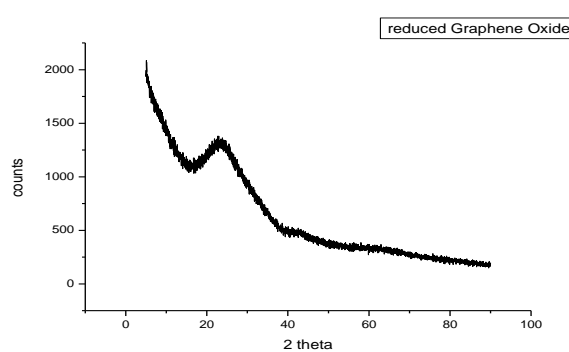


Fig 3.1.2: XRD of Graphene

a. *Characterization of Graphene-TiO<sub>2</sub> nano composite*

The crystalline phase of TiO<sub>2</sub>-graphene nanocomposite was determined by powder X-ray diffraction (XRD). As shown in Fig.3.2.1, the XRD patterns can be indexed to the anatase TiO<sub>2</sub> phase (JCPDS file no. 89-4921), suggesting the complete formation of anatase TiO<sub>2</sub> during the hydrothermal process. The high intensity and the

small width at the half height of the diffraction peaks indicate the big crystallized portion of the  $\text{TiO}_2$  particles on the surface of graphene. However, the diffraction peaks of graphene are not distinguishable in XRD patterns of the nanocomposite, which might be ascribed to their low diffraction intensity and shielding of the graphene peaks by those of  $\text{TiO}_2$ .

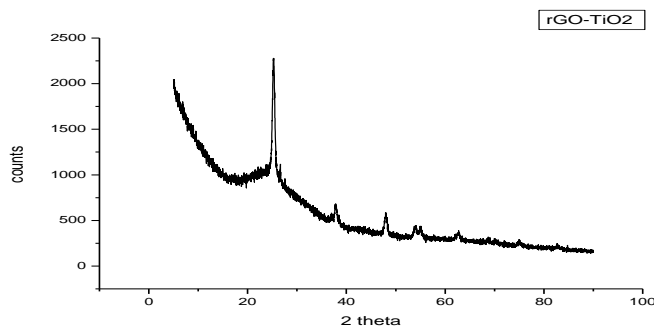


Fig 3.2.1: XRD of Graphene- $\text{TiO}_2$  nano composite

The SEM image of the  $\text{TiO}_2$ -graphene is given in Fig 3.2.2. It can be seen that  $\text{TiO}_2$  was formed in a highly faceted morphology on the substrates of graphene with ca. 50–100nm diameter for the clusters. The structure characterization results suggest that hydrothermal reaction proceeded with efficient crystallization of  $\text{TiO}_2$  in anatase phase and their in situ immobilization on graphene substrate.

TEM analysis revealed a homogeneous distribution of  $\text{TiO}_2$  nano particles at the surface of graphene shown in figure 3.2.3. From the images we can observe that graphene is composed of well dispersed  $\text{TiO}_2$  nano particles with dark regions showing partly agglomerated nano particles

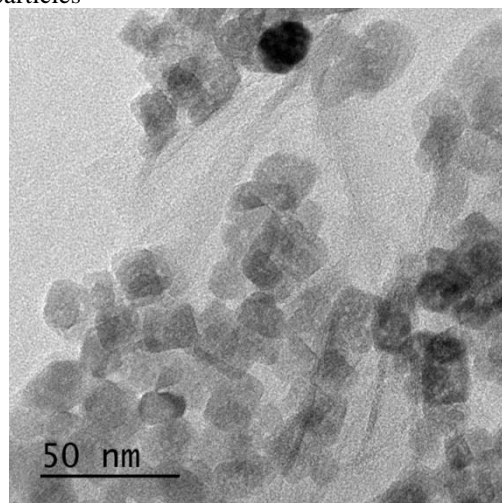
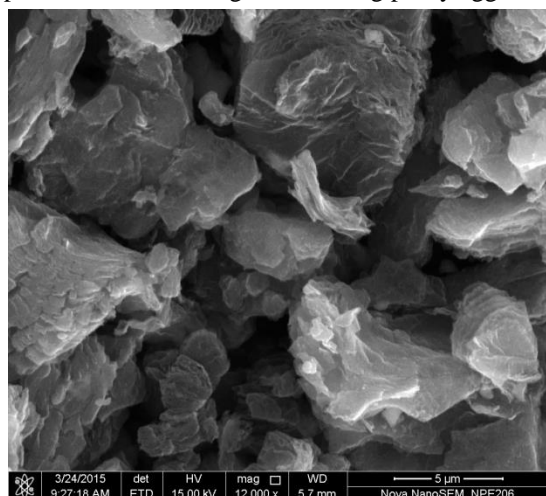


Fig 3.2.2: SEM images of Graphene- $\text{TiO}_2$  nano composite Fig 3.2.3: TEM images of Graphene- $\text{TiO}_2$  nano composite

### 3.3. Electrochemical response of Dopamine Towards Modified electrodes

The electrochemical behaviour of Dopamine at Bare GCE, GR/GCE and GR- $\text{TiO}_2$ /GCE was investigated and the results are shown in figure 6. The peak potential of GR- $\text{TiO}_2$ /GCE is lower than the peak potential of GR/GCE. It is

shown that a pair of redox peak appears at the typical CV at GR-TiO<sub>2</sub>/GCE electrodes in the potential range at a scan rate of 100mV/s are shown in fig 3.3.1. This suggest the sunnergistic effect of GR-TiO<sub>2</sub> nanocomposite provides an efficient micro environment for the electrochemical reaction of Dopamine.

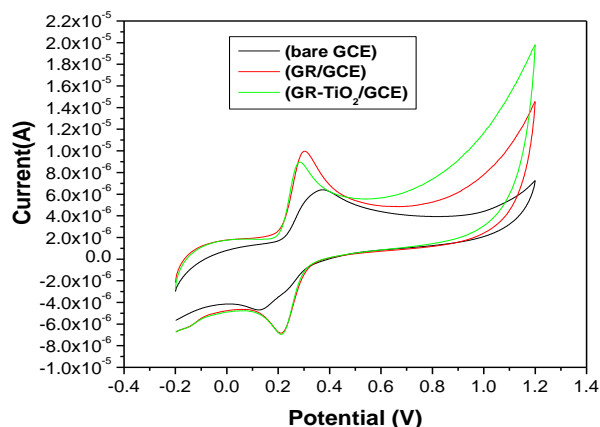


Fig 3.3.1. Cyclic Voltammograms of  $2 \times 10^{-4}$  M Dopamine at Bare GCE, GR/GCE and GR-TiO<sub>2</sub>/GCE in 0.1M PBS (pH 7)

### 3.4. The influence of pH on the electrolytic oxidation of DA

For the determination of a compound by cyclic voltammetry or differential pulse voltammetry, it is very essential to optimise certain measurement parameters. The following discussions deal with the optimisation of each one of these parameters in the context of detecting DA. The first thing to do in a voltammetric determination is to select the potential window. The initial and final potential values are selected in such a way that the redox potential of the analytes lie in between this range. Particular concentration of the analysis that give obvious peaks during a voltammetric determination are selected for further investigations on optimising pH and scan rate. For simultaneous determinations of two or more samples, their selected concentrations should not cause mutual interference too. Figure 3.4.1 shows the effect of pH on the current response of Dopamine on the GR-TiO<sub>2</sub>/GCE electrode. The oxidation peak current gradually increased with increase of pH values from 3 to 5, then the oxidation peak current decreases from 5-8. Therefore considering the sensitivity pH 5 was taken for the subsequent experiments.

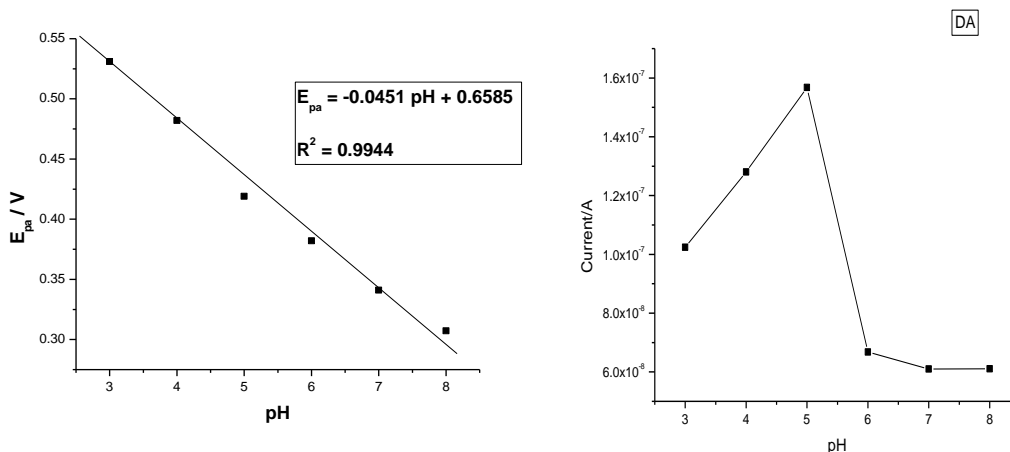


Fig 3.4.1: Cyclic Voltammograms of Dopamine at different pH

3.5. Effect of scan rate on the detection of Dopamine at modified electrode

To further investigate the electrochemical kinetics at the composite electrode, CV's were recorded at various scan rates. Both anodic and cathodic peak currents increases with scan rate. The voltametric peak currents increases with increase of square root of scan rate, ie peak current proportional to  $v^{1/2}$  indicates that the electron transfer at the electrode is controlled by diffusion which is ideal condition for a qualitative analysis and peak appears begins to increase with increase in scan rate indicating a quazi reversible reaction. This indicates that the rate determining step of the redox reaction of DA at the TiO<sub>2</sub>-GR/GCE involves only one proton and one electron. Thus the overall oxidation of DA takes place in two mono electronic steps.

Figure 3.5.1 shows the CV curves with scan rates of 10, 100, 200, 300, 400, 500, 600, 700, 800, 900 and 1000 mV/s resp. The oxidation peak current increased gradually with the scan rate. Figure 3.5.2 shows the linearity obtained for the relation between redox peak currents and the square root of scan rate. It shows a linear range from 10mV/s to 1000mV/s with a correlation of 0.9984. This indicates the redox reaction of DA exhibit a diffusion controlled nature at TiO<sub>2</sub>-GR/GCE. To get information about the rate determining step, the Tafel plot was drawn [figure 3.5.3].

From the equation

$E_{pa} = 2.303RT/2(1-\alpha)nF \log v + \text{constant}$ , if the value of the electron transfer coefficient ( $\alpha$ ) was assumed to be equal to 0.5, then  $n$  was equal to be 1.23.

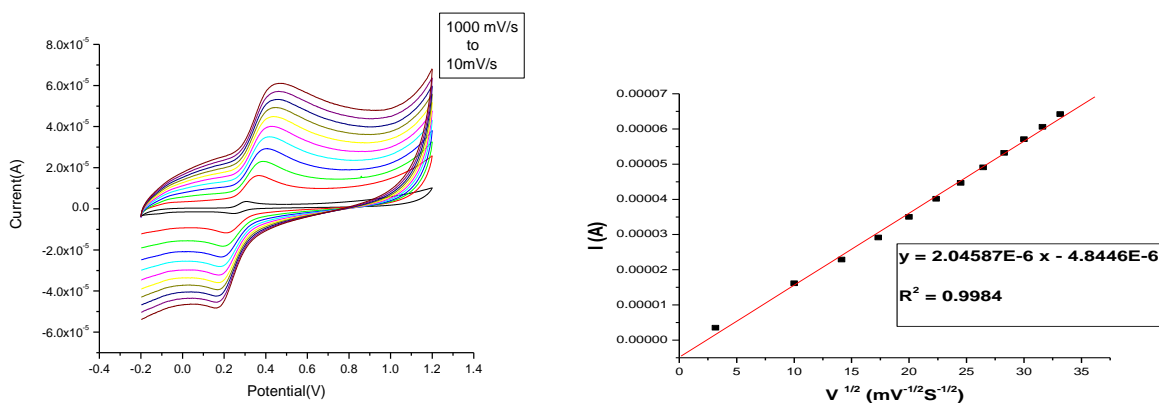


Fig 3.5.1 : Variation of peak current of Dopamine with Different Scan rates from 10mV/s to 1000mV/s

Fig 3.5.2 : Variation of peak current of Dopamine with square root of scan rates from 10mV/s to 1000mV/s

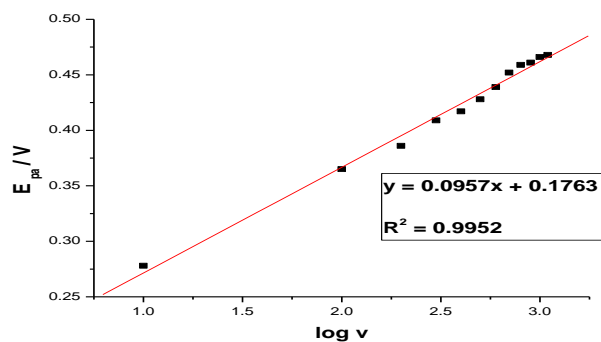


Fig 3.5.3 : Tafel plot

### 3.6. Selective detection DA using GR-TiO<sub>2</sub>/GCE electrode

Addition of Gr-TiO<sub>2</sub> on the galssy carbon electrode makes roughness on the modified surface; adsorption and the rate of electron transfer are much enhanced at the modified electrode compared to the bare GCE. Because of the comparatively stronger adsorption of DA, Differential Pulse Voltammetry technique was used for the selective detection of Dopamine at GR-TiO<sub>2</sub>/GCE electrode. DPV have much higher current sensitivity and better resolution than CV. DPV was used to investigate the relationship between peak currents and Dopamine concentrations under the required conditions. The figure 3.6 shows the DPVs of varying concentrations of DA from  $2 \times 10^{-8}$  to  $2 \times 10^{-6}$  mol/L in 0.1M PBS (pH 7) at the GR-TiO<sub>2</sub>/GCE. The results show a linear relationship between peak currents and Dopamine concentrations within the range from  $2 \times 10^{-8}$  to  $2 \times 10^{-6}$  mol/L with a correlation coefficient of 0.997 and the detection limit was obtained as 54nM.

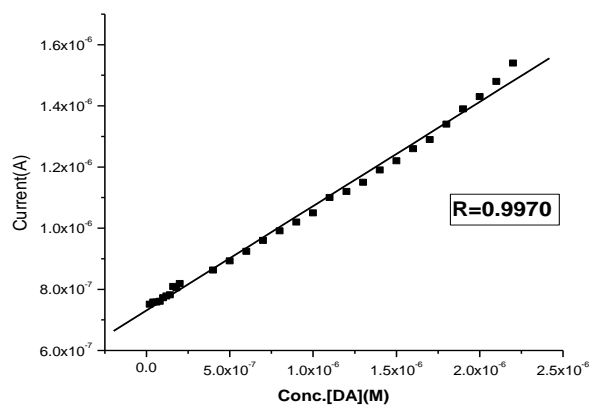


Fig 3.6.1: DPV of Dopamine at different concentrations

### 3.7. Selective detection of Dopamine in presence of Ascorbic acid and Uric acid

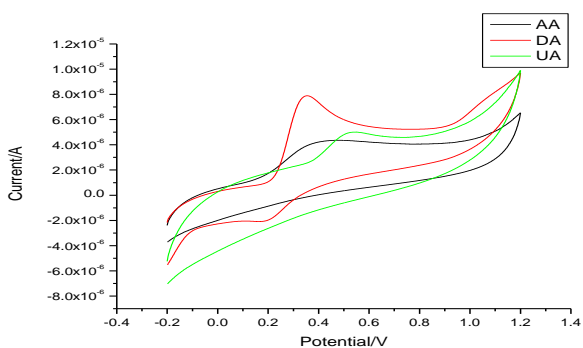


Fig3.7.1: CV s of DA(0.5mM),AA (0.5mM) and UA(0.5mM) at TiO<sub>2</sub>-Gr-GCE in 0.1M PBS(PH 7) at 100mV/S scan rate

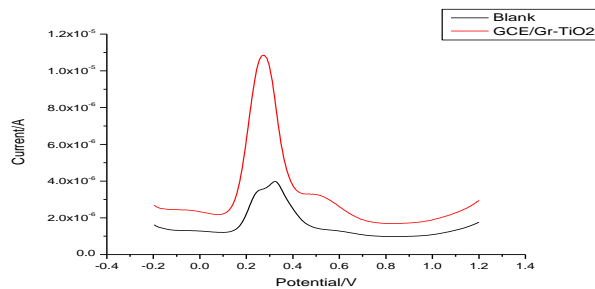


Fig3.7.2.: DPV s at bare GCE and TiO<sub>2</sub>-Gr-GCE in 0.1M PBS(PH 7) contains DA(40x10<sup>-6</sup>M),AA (1mM) and UA (50x10<sup>-6</sup>M)

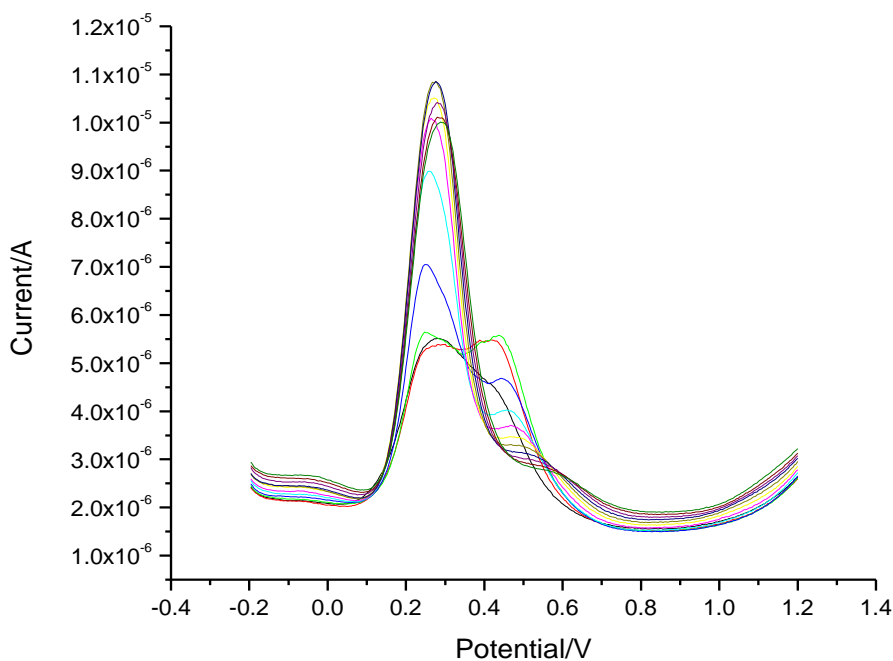


Fig 3.7.3: DPV s of 5, 10, 20, 40, 60, 80, 100, 120, 140, 160, 180 micro M DA at TiO<sub>2</sub>-Gr-GCE in the presence of 1mM AA and 100 microM UA in 0.1M PBS(Ph 7) amplitude 100mv

Figure 3.7.1 represents the voltametric response of DA,UA and AA at the TiO<sub>2</sub>-Graphene-GCE. Among the three species AA is the most inactive one. DA shows both anodic and cathodic peak currents. This suggest that the TiO<sub>2</sub> – Graphene modified electrode shows more catalytic activity towards DA in comparison with AA and UA. Figure



3.7.2 shows that voltametric response of the ternary mixture at the bare GCE is an overlapped peak indicating poor selectivity, but at the TiO<sub>2</sub>-Gr-GCE peaks of the species are well resolved indicating very good selectivity. Figure 3.7.3 represents the DPV peak currents of DA increases linearly with the increase in concentration of DA which suggests the AA and UA have no interference for the determination DA.

### 3.8. Real sample analysis

To study about the applicability of the developed sensor, the electrode was tested for the determination of DA in Injection samples. Recovery determined by spiking DA solution was found to be in the range of 98-101 % indicating the practical applicability of the modified electrode.

## IV. Conclusion

An electrochemical sensor GR-TiO<sub>2</sub> modified electrode was prepared for the detection Dopamine. We successfully synthesised the graphene-TiO<sub>2</sub> nanocomposite by the hydrothermal treatment. The crystallinity and crystalline size were examined by XRD and TEM. The surface morphology of the nanocomposite is examined by SEM. The crystalline size of the as prepared nanocomposite was 17nm. The sensor exhibited good sensitivity of dopamine with the detection limit of 54nM by DPV.

## Acknowledgements

I express my sincere thanks to Department of Chemistry, SNCW for giving the facilities for the completion my work.

## References

1. W. Choi, I. Lahiri, R. Seelaboyina and Y.S. Kang, *Crit. Rev. Solid State Mater. Sci.*, 35, 2010, 52.
2. D.K. Kampouris and C.E. Banks, *Chem. Commun. (Camb.)*, 46, 2010, 8986.
3. S. Wu, Q. He, C. Tan, Y. Wang and H. Zhang, *Small*, 9, 2013, 1160.
4. A. Ambrosi, C.K. Chua, A. Bonanni and M. Pumera, *Chem. Rev.*, 114, 2014, 7150.
5. W. Yuan, Y. Zhou, Y. Li, C. Li, H. Peng, J. Zhang, Z. Liu, L. Dai and G. Shi, *Sci. Rep.*, 3, 2013, 2248.
6. D.A. Brownson, L.J. Munro, D.K. Kampouris and C.E. Banks, *RSC Advances*, 1, 2011, 978.
7. D.A. Brownson, C.W. Foster and C.E. Banks, *Analyst (Lond.)*, 137, 2012, 1815.
8. M. Pumera, *Chem. Soc. Rev.*, 39, 2010, 4146.
9. X. Chen, G. Wu, Y. Jiang, Y. Wang and X. Chen, *Analyst (Lond.)*, 136, 2011, 4631.
10. M. Zhou, Y. Zhai and S. Dong, *Anal. Chem.*, 81, 2009, 5603.
11. P.V. Kamat, *J. Phys. Chem. Lett.*, 1, 2010, 520.
12. D. Chen, L. Tang and J. Li, *Chem. Soc. Rev.*, 39, 2010, 3157.
13. M. Pumera, *Chem. Soc. Rev.*, 39, 2010, 4146.
14. Y. Shao, S. Zhang, C. Wang, Z. Nie, J. Liu, Y. Wang and Y. Lin, *J. Power Sources*, 195, 2010, 4600.
15. H. Zhang, X. Lv, Y. Li, Y. Wang and J. Li, *ACS Nano*, 2010, 4380.
16. L. Dong, R.R.S. Gari, Z. Li, M.M. Craig and S. Hou, *Carbon*, 48, 2010, 781.
17. S. Guo, D. Wen, Y. Zhai, S. Dong and E. Wang, *ACS Nano*, 4, 2010, 3959.
18. C. Shan, H. Yang, D. Han, Q. Zhang, A. Ivaska and L. Niu, *Biosens. Bioelectron.*, 25, 2010, 1070.
19. Y. Li, L. Tang and J. Li, *Electrochem. Commun.*, 11, 2009, 846.
20. Y. Zhang, H. Li, L. Pan, T. Lu and Z. Sun, *J. Electroanal. Chem.*, 634, 2009, 68.
21. D. Wang, D. Choi, J. Li, Z. Yang, Z. Nie, R. Kou, D. Hu, C. Wang, L.V. Saraf, J. Zhang, I.A. Aksay and J. Liu, *ACS Nano*, 3, 2009, 907.
22. K. Wang, Q. Liu, X.Y. Wu, Q.M. Guan and H.N. Li, *Talanta*, 82, 2010, 372.
23. E. Topoglidis, C.J. Campbell, A.E.G. Cass and J.R. Durrant, *Langmuir*, 17, 2001, 7899.
24. S. Liu and A. Chen, *Langmuir*, 21, 2005, 8409.
25. A. Liu, M. Wei, I. Honma and H. Zhou, *Adv. Funct. Mater.*, 16, 2006, 371.
26. S.J. Bao, C.M. Li, J.F. Zang, X.Q. Cui, Y. Qiao and J. Guo, *Adv. Funct. Mater.*, 18, 2008, 591.
27. Y. Luo, H. Liu, Q. Rui and Y. Tian, *Anal. Chem.*, 81, 2009, 3035.
28. H. Lin, X. Ji, Q. Chen, Y. Zhou, C.E. Banks and K. Wu, *Electrochem. Commun.*, 11, 2009, 1990.
29. Y. Luo, Y. Tian, A. Zhu, Q. Rui and H. Liu, *Electrochem. Commun.*, 11, 2009, 174.
30. N.F. Atta, A. Galal, F.M. Abu-Attia and S.M. Azab, *J. Mater. Chem.*, 21, 2011, 13015.
31. X. Xu, H. Zhang, H. Shi, C. Ma, B. Cong and W. Kang, *Anal. Chem.*, 427, 2012, 10–17.
32. V. Carrera, E. Sabater, E. Vilanova, M. A. Sogorb, *J. Chromatogr. B: Anal. Technol. Biomed. Life Sci.*, 847, 2007, 88–94.
33. K. Vuorensoja, H. Siren and U. Karjalainen, *J. Chromatogr. B: Anal. Technol. Biomed. Life Sci.* 893-894, 2012, 92-100.
34. Y. Liu, J. Huang, H. Hou and T. You, *Electrochem. Commun.*, 10, 2008, 1431–1434.
35. N. Boes and H. Z. Uchner, *J. Less-Common Met.*, 49, 1976, 223–240.

36. E. Palecek, *Talanta*, 56, 2002, 809–819.
37. Y. Guan, Q. Chu, J. Ye, *Anal. Bioanal. Chem.*, 380, 2004, 913-917.
38. Z. Wang, Y. Wang, G. Luo, *The analyst*, 127, 2002, 1353-1358.
39. D. Martin-Perez, M. L. Ferrer, C.R. Mateo, *Anal. Biochem.*, 322, 2003, 238-242.
40. K. Innoue, T. Namiki, Y. Iwasaki, Y. Yoshimura, H. Nakazawa, *J. Chromatogr. B*, 785, 2003, 57-63.
41. Filisitti, Cozi, TMCC, N. C. Carpita, *Anal. Biochem.*, 197, 1991, 157-162.
42. H.C. Hong, H.J. Huang, *Anal. Chim. Acta.*, 499, 2003, 41-46.
43. M. Pumera, *Chem. Soc. Rev.*, 39, 2010, 4146–4157.
44. X. Chen, G. Wu, Y. Jiang and Y. Wang, *Analyst.*, 136, 2011, 4631–4640.
45. M. Zhou, Y. Zhai and S. Dong., *Anal. Chem.*, 81, 2009, 5603–5613.
46. F. Li, J. Chai, H. Yang, D. Han and L. Niu, *Talanta.*, 81, 2010, 1063–1068.
47. Y. Fan, H. T. Lu, J.H. Liu, C.P. Yang, Q.S. Jing, Y.X. Zhang, X. K. Yang and K.J. Huang., *Colloids Surf. B*, 83, 2011, 78–82.
48. D. Han, T. Han, C. Shan, A. Ivaska and L. Niu, *Electroanalysis*, 22, 2010, 2001–2008.
49. M. Li, J.E. Zhu, L. Zhang, X. Chen, H. Zhang, F. Zhang, S. Xu and D. Evans, *Nanoscale*, 3, 2011, 4240–4246.
50. N. Zhang, H. Qiu, Y. Liu, W. Wang, Y. Li, X. Wang, J. Gao, *J. Mater. Chem.*, 21, 2011, 11080-11083.
51. M. Mallesha, R. Manjunatha, C. Nethravathi, M. Rajamathi, J.S. Melo and T.V. Venkatesha, *sensors and actuators B*, 81, 2011, 104–108.
52. Z.H. Sheng, X.Q. Zheng, J.Y. Xu, W.J. Bao, F.B. Wang and X.H. Xia, *Biosens. Bioelectron*, 34, 2012, 125–131.